

# The Electric Dipole Array: An Attempt to Match the Ideal Current Pattern for Central SNR at 7 Tesla

Graham Charles Wiggins<sup>1</sup>, Bei Zhang<sup>1</sup>, Riccardo Lattanzi<sup>1</sup>, Gang Chen<sup>2</sup>, and Daniel Sodickson<sup>1</sup>

<sup>1</sup>The Bernard and Irene Schwartz Center for Biomedical Imaging, NYU Medical Center, New York, NY, United States, <sup>2</sup>The Sackler Institute of Graduate Biomedical Science, NYU School of Medicine, New York, NY, United States

**Introduction:** The analysis of the Ultimate Intrinsic SNR (UISNR) through a current mode expansion employing dyadic Green's functions (DGF) [1,2] makes it possible to plot the receive current pattern on a given surface which would result in the UISNR for a given position in the phantom, that is, the ideal current pattern [1,3]. For a cylindrical phantom with a concentric cylindrical surface, the ideal current pattern which maximizes central SNR looks like a pair of distributed loops at low field (Fig. 1 left). At high fields, however, the ideal current pattern for central SNR assumes a pattern that is a mixture of loops and electric dipole components [3]. It has been shown that the contribution of the latter to UISNR increases with frequency [3,4] and, for certain geometries, the ideal current pattern can be dominated by electric dipole currents, in which the current flows in straight lines along the length of the cylinder with no return path (Fig. 1 right). The most common antenna structure for MRI is the surface coil loop, but this analysis suggests that at high field an electric dipole structure might become more optimal. Although conventional stripline coils or TEM elements may appear to have a similar current pattern, both rely on the presence of a closely coupled shield which provides a return path and hence differs from the simulated structure where current can flow only on one surface. To mimic the ideal current pattern we propose the use of an array of dipole antennas. Dipole antennas are usually eschewed for MRI on the basis that they are efficient generators of electric fields, and should increase receive noise and transmit heating. Electric dipole antennas arrays are in fact used for hyperthermia therapy to steer heating into deep tissues [5]. Given the testimony of the ideal current patterns, however, it would appear that there are regimes where electric dipole currents may provide superior performance than conventional loops. We therefore constructed an array of 8 dipole antennas on a cylinder and compare it to conventional coil designs for 7 Tesla imaging.

**Methods:** For a simple dipole antenna, maximum efficiency is achieved when the length of the antenna is equal to  $\frac{1}{2}$  the free space wavelength of the electromagnetic wave that is to be transmitted or received. For 7 Tesla, this corresponds to a length of  $\sim 50$  cm, which is not practical for most applications. The dipole antenna may be shortened with some loss of efficiency by adopting the folded dipole design (Fig. 2). This antenna differs from the radiative antenna [6] in that it does not rely on a thick high-dielectric substrate, which would negate direct comparison to the simulated ultimate current patterns. Two different coils were constructed on identical 15.2 cm diameter cylindrical formers— an 8 element folded dipole array and an 8 element capacitively decoupled array. A cylindrical phantom with 6 cm inner diameter and 24 cm length was filled with a mixture with  $\epsilon_r = 57.5$  and  $\sigma = 0.8$ , approximating average tissue properties at 7 T. The dipole elements were matched to 50  $\Omega$  coax using the circuit depicted in Figure 3. For the capacitively decoupled loops the coax signal and ground were connected to either side of one of the capacitors in the loop, whose value was adjusted to provide a 50  $\Omega$  match. A coaxial cable trap was placed by each match capacitor in the loop array to minimize common mode cable currents. For imaging, RF transmit power was equally divided with an 8-way splitter (Werlatone, Patterson NY) and delivered to the coil elements through an in-house built T/R switch and preamp interface. Signals from all 8 elements were recorded and reconstructed before being combined as the root sum of squares (RSS). All imaging data were acquired on a 7 T scanner (Siemens Healthcare, Erlangen Germany)

$B_1^+$  efficiency was determined by using a turbo-FLASH sequence with various preparations pulses to find the RF voltage required to produce a 90 degree flip angle in the center of the phantom [7].  $B_1^+$  maps were generated using a similar approach embodied in a manufacturer works-in-progress sequence (Siemens Healthcare, Erlangen Germany). To measure SNR, a gradient echo sequence was acquired (TR/TE/Flip/BW/slice = 200/4.07/20°/300/3mm, Matrix = 256, FoV = 220mm) both with and without RF excitation and SNR maps were generated according to the method described in reference 8.

**Results:** The dipole array exhibited strong coupling between nearest neighbors of  $\sim 8$  dB. The folded dipole elements are very sensitive to proximity to the sample, exhibiting strong frequency shifts. With the fixed coil to phantom relationship we were nevertheless able to tune and match each element to better than -19dB. The capacitively decoupled array was also strongly coupled, with -11 dB between neighboring elements, but could still be well matched at each port. To achieve a calibrated flip angle in the center of the phantom the scanner transmitter reference voltages were 137 and 106v respectively. The excitation pattern produced by each coil was a nearly identical standard birdcage pattern (not shown). The SNR for each coil is shown in Figure 4. The dipole array SNR is only 75% that of the conventional array. More interesting behavior emerges when we examine the  $B_1^+$  profiles of the individual elements (Fig. 5). There is little evidence of the familiar twisting of the  $B_1^+$  profile with the dipole element, just a slight bias to one side. In this regard the dipole elements are similar to the radiative antenna [6]. The loop elements on the other hand show strong asymmetry and multiple lobes, as is more usual.

**Discussion:** We have so far not evaluated the SAR characteristics of the two coil arrays, which will be of interest since electric dipoles may be expected to produce more heating. We have however simulated a head sized birdcage with a shield and an 8 element dipole array of identical dimensions, also in a shield. The results are shown in Figure 6. The dipole array produces much higher  $B_1^+$  per watt of input power, but also produces significantly more heating. Using  $(B_1^+)^2 / \text{Peak SAR}$  as a performance metric, this dipole array is 25% less efficient than the birdcage. Thus initial experiments using an array of electric dipole antennas to mimic the ideal current patterns have not produced a performance gain. More recently we repeated the ideal current pattern simulation for the exact geometries of the coils and phantoms here, and found that they are in fact still dominated by loop-like currents. Performance gain from the use of dipole antennas will depend on specific coil and sample geometry and field strengths. Better still, if dipole elements can be combined with loop elements the full diversity of the high field ideal current patterns could be captured, hopefully leading to a significant performance gain.

[1] Lattanzi R. (2008) ISMRM p.78 [2] Lattanzi R. (2010) NMR Biomed 23(2):142-51 [3] Lattanzi R. (2011), ISMRM p.3876 [4] Schnell W. (2000), IEEE Trans Ant Prop 48:418-28.[5] Issels R. Lancet Oncology 2010;11:561-70 [6] Raaijmakers A. MRM 2011 Nov;66(5):1488-9[7] Breton E. NMR Biomed. 2010 May;23(4):368-74 [8] Kellman P. MRM 54:1439–1447 (2005)

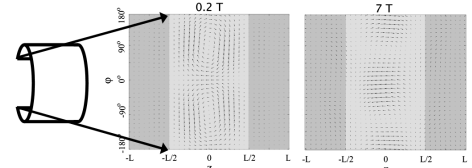


Figure 1: Ideal Current patterns for 40 cm dia. Phantom and 44cm dia. coil at low and high field

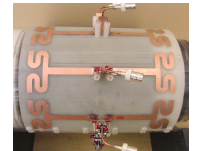


Figure 2: Folded dipole array

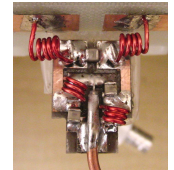


Figure 3. Match Circuit

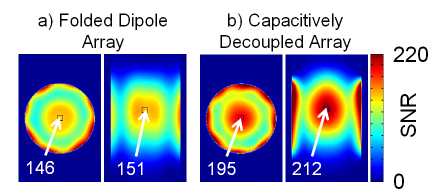


Figure 4. SNR in axial and coronal planes

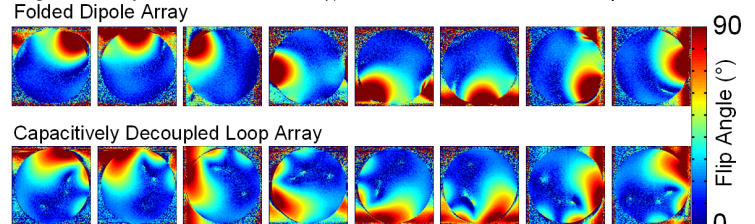


Figure 5. Flip angle maps for individual elements of the two arrays

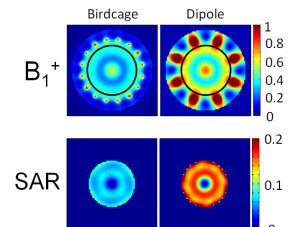


Figure 6 Simulations of head sized coils